PNC TN8410 97-071

COUPLED THERMO - HYDRO - MECHANICAL
EXPERIMENT AT KAMAISHI MINE

TECHNICAL NOTE 11-96-04

FUNDAMENTAL PROPERTIES OF BENTONITE OT-9607

T. Fujita, M. Chijimatsu and H. Ishikawa
Power Reactor and Nuclear Fuel Development Corporation (PNC)
H. Suzuki and K. Matsumoto
Inspection and Development Corporation

公　開　資　料
PNC TN8410 97-071
１９９７年２月

釜石原位置試験場における粘土充填・熱負荷試験
テクニカルノート　11-96-04
ベントナイトOT-9607の基本特性

藤田朝雄*1・鈴木英明*2・松本一浩*2・千々松正和*1・石川博久*1

要　旨

地層処分における技術開発の観点からは、工学規模での試験によるニアフィールド環境である周辺岩盤の挙動が人工バリアに与える影響の把握および周辺岩盤を含むニアフィールド性能の定量的評価と室内および原位置における大型試験による人工バリアの品質性能の確認を行い、地層処分技術の信頼性向上を図ることが重要となっている。そのため、動力炉・核燃料開発事業団東海事業所の地層処分基盤研究施設等における工学規模の試験と並行して、原位置試験場において、人工バリアの品質性能の確認およびその実岩盤条件下でのニアフィールド連成挙動を評価することが必要となっている。

そこで、実条件でのニアフィールド環境を把握するため釜石原位置試験場において粘土充填・熱負荷試験を実施している。

本試験では緩衝材としてベントナイトOT-9607を使用した。これはベントナイトクニゲルＶ１の製造過程において精製される粒状のベントナイトである。本論では、本材料を用いた理由及びその基本特性について論ずる。

---

*1 東海事業所　環境技術開発部　地層処分開発室

*2 （株）検査開発

PNC TN8410 97-071
February, 1997

COUPLED THERMO-HYDRO-MECHANICAL EXPERIMENT AT KAMAISHI MINE

TECHNICAL NOTE 11-96-04

FUNDAMENTAL PROPERTIES OF BENTONITE OT-9607

ABSTRACT

It is an important part of the near field performance assessment of nuclear waste disposal to evaluate coupled thermo-hydro-mechanical (T-H-M) phenomena, e.g., thermal effects on groundwater flow through rock matrix and water seepage into the buffer material, the generation of swelling pressure of the buffer material, and thermal stresses potentially affecting porosity and fracture apertures of the rock. An in-situ T-H-M experiment named 'Engineered Barrier Experiment' has been conducted at the Kamaishi Mine, of which host rock is granodiorite, in order to establish conceptual models of the coupled T-H-M processes and to build confidence in mathematical models and computer codes.

We used the BENTONITE OT-9607 as a buffer material. This is the special order goods for this experiment and the granulated bentonite before final crush of KUNIGEl V1.

This note describes the reason for using this material and the fundamental properties.

COUPLED THERMO-HYDRO-MECHANICAL EXPERIMENT AT KAMAISHI MINE

TECHNICAL NOTE 11-96-04

FUNDAMENTAL PROPERTIES OF BENTONITE OT-9607

CONTENTS

1. INTRODUCTION

The coupled thermo-hydro-mechanical (T-H-M) experiment in situ has been carried out as a task of Kamaishi in-situ experiments in order to establish the coupled T-H-M conceptual models and to build up confidence to the mathematical models and computer codes [1].

The Kamaishi Mine is located approximately 600km north of Tokyo. The bedrock in this area consists of Paleazoic sedimentary rock, Cretaceous sedimentary rock and igneous complexes. The facilities of T-H-M experiment are located at a drift 550m above sea level (EL 550m drift) in the Cretaceous-age Kurihashi granodiorite.

The program of T-H-M experiment is divided into five phases; Excavation of Drifts, Measurement of Rock Properties, Excavation of Test Pit, Setting up of Bentonite, and T-H-M test.

In order to understand and to model T-H-M behavior of bentonite in the T-H-M experiment, it is necessary to measure and represent quantitatively the relevant characteristics of the bentonite.

Measurements of hydraulic, thermal and mechanical properties of bentonite at laboratory were carried out. This report describes the fundamental properties of the bentonite used in the T-H-M experiment at the Kamaishi mine.

2. BENTONITE OT-9607

2.1 PRODUCTION

The BENTONITE OT-9607 (OT-9607) is natural sodium bentonite provided by Kunimine Industries Co., Ltd. Figure 2.1 shows production flow of the OT-9607. At first the source mineral of bentonite is crushed roughly after carrying into the plant. The bentonite is crushed finely after drying. The crashed bentonite is classified according to a particle size and that of a particle size under 2 mm is collected as the OT-9607. The bentonite under 250 mesh is collected as the bentonite Kunigel V1™ [2] after crushing again.

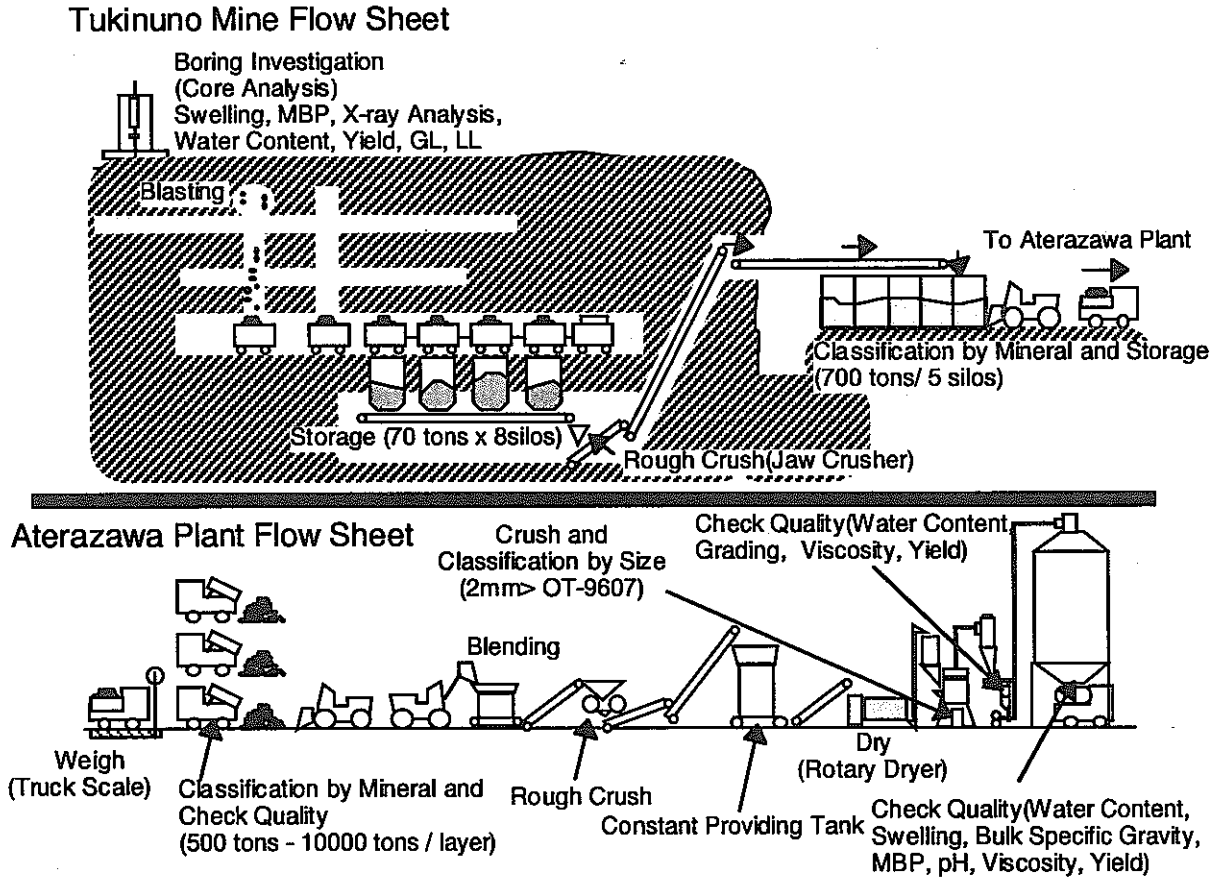

Figure 2.1 Production flow of the OT-9607

Because methylene blue is selectively adsorbed to montmorillonite, the montmorillonite content can be estimated by comparing methylene blue exchange capacity of bentonite with that of pure bentonite. The measured methylene blue exchange capacity of the OT-9607 are summarized in Table 2.1. The estimation of montmorillonite content of the OT-9607 is described with those of Kunigel V1 and Kunipia™ [2] which is a purified Na-bentonite in Table 2.2. The montmorillonite content of the OT-9607 is slightly smaller than that of the Kunigel V1. Because the Kunigel V1 is produced by crushing the OT-9607 and the impurity is eliminated from the OT-9607.

Table 2.1 Measured methylene blue exchange capacity of the OT-9607

Number	Methylene blue exchange capacity [mmol/100g]			
	Maximum	Minimum	Mean	Standard deviation
16	68	60	63.5	2.48

Table 2.2 Estimation of montmorillonite content

	OT-9607	Kunigel V1	Kunipia
Methylene blue exchange capacity [mmol/100g]	63.5	66.0	136.0
Montmorillonite content [%]	45.5	47.3	97.5

The grain size accumulation curves of the OT-9607 and the Kunigel V1 are shown in Figure 2.2. The OT-9607 is the maximum grain size of 4.75 mm, the gravel fraction of 0.2 %, the sand fraction of 92.8 %, the silt fraction of 7.0 % and the uniformity coefficient of 4.8.

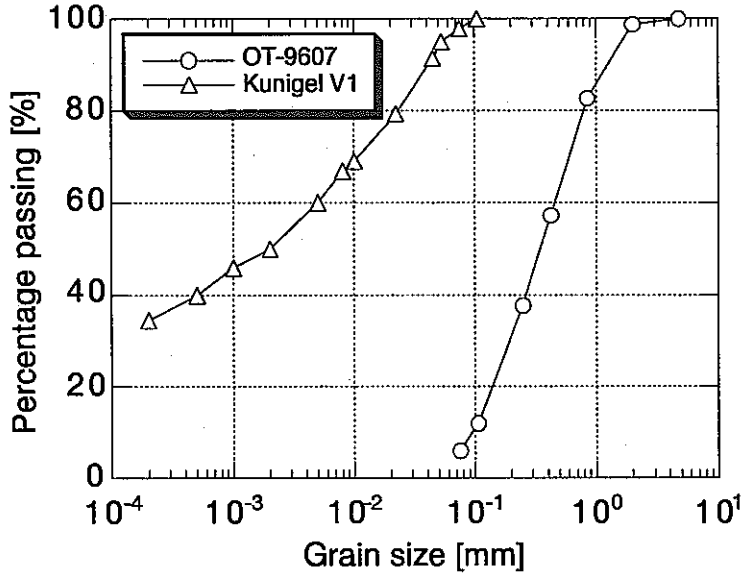

Figure 2.2 Grain size accumulation curves of the OT-9607 and the Kunigel V1

2.2 COMPACTION TEST

The compaction curves obtained from the compaction test using a rammer for the OT-9607 and the Kunigel V1 are shown in Figure 2.3. As the compaction energy increases, the maximum dry density increases and the optimum moisture content decreases. The dry density of OT-9607 is large compared to that of Kunigel V1 for the same compaction energy.

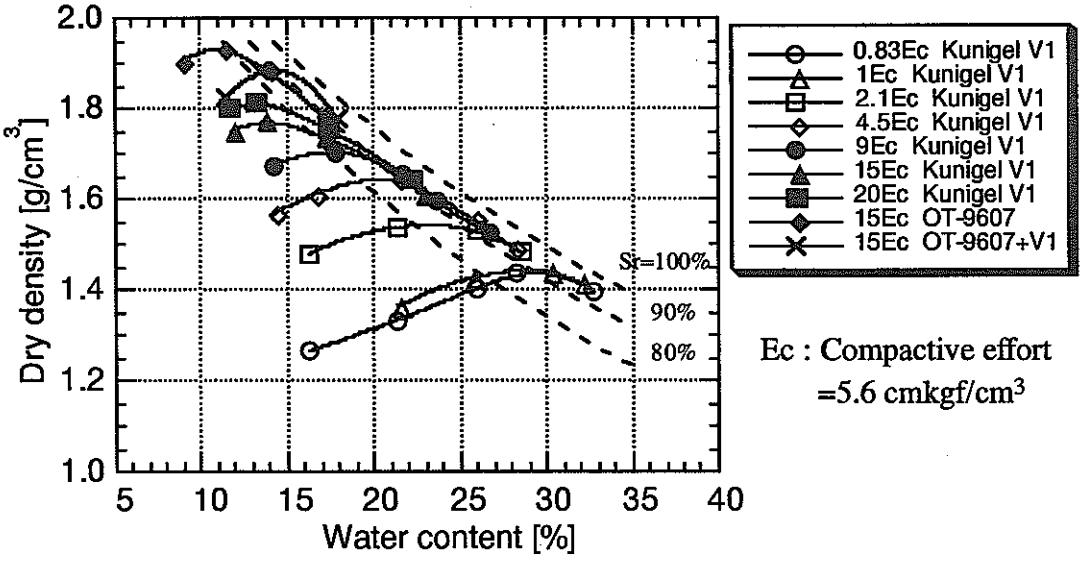

Figure 2.3 Compaction curves obtained from the compaction test

3. LABORATORY TEST

3.1 WATER MOVEMENT

3.1.1 WATER MOVEMENT IN SATURATED STATE

The hydraulic conductivity k of a porous medium is determined from the volumetric flow rate q and the hydraulic gradient i according to the Darcy's law.

$$q = kAi \tag{3.1}$$

where A is the cross-sectional area. The intrinsic permeability κ [3] of the medium is calculated from the hydraulic conductivity using

$$k = \kappa\rho g / \mu \tag{3.2}$$

where ρ is the density of water, μ is the viscosity of water and g is the gravitational constant. The intrinsic permeability is said to depend solely on properties of the solid matrix such as grain size distribution, shape of grains, tortuosity, specific surface, and porosity.

Three samples were compacted uniaxially and statically to a dry density of 1.65 g/cm^3 in rigid stainless steel cells, shown in Figure 3.1, for constant-head permeability tests. The diameter of the cells was 50 mm and the thickness of the compacted specimens was 5 mm. Distilled water pressurized by compressed air was supplied into the cell, and the volumetric flow rate was determined by weighing the effluent as a function of time. The pressure of the compressed air was maintained at 0.8 MPa during the tests, that is the hydraulic gradient applied to the specimens was 16000. In this study, the following heating procedure for each bentonite specimen with a thermostat was adopted; 25°C→60°C→90°C.

Measured results of the hydraulic conductivities increased during the heating period for all specimens as shown in Figure 3.2. The calculated results with equation (3.2) of the intrinsic

permeability of the specimens are shown in Figure 3.3. The intrinsic permeability of which the mean is 1.60×10^{-20} m^2 has a tendency to be independent of temperature. Table 3.1 summarizes the measured hydraulic conductivities and the calculated intrinsic permeabilities.

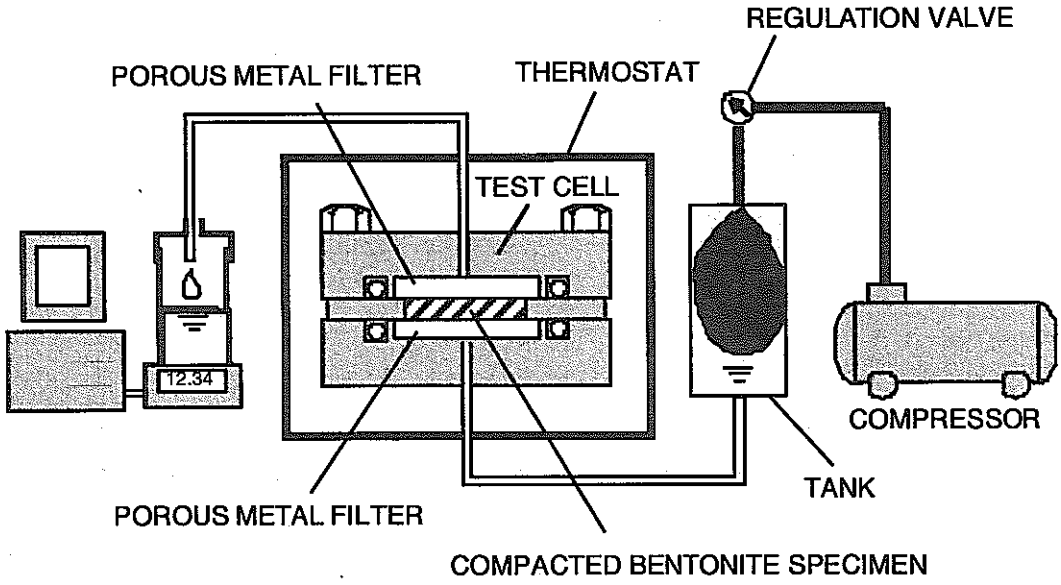

Figure 3.1 Schematic of test apparatus of hydraulic conductivity

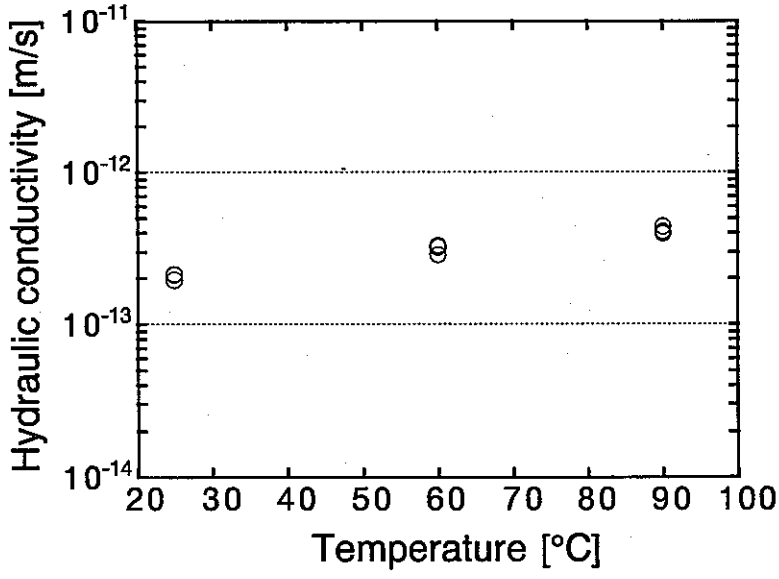

Figure 3.2 Relation between hydraulic conductivity and temperature

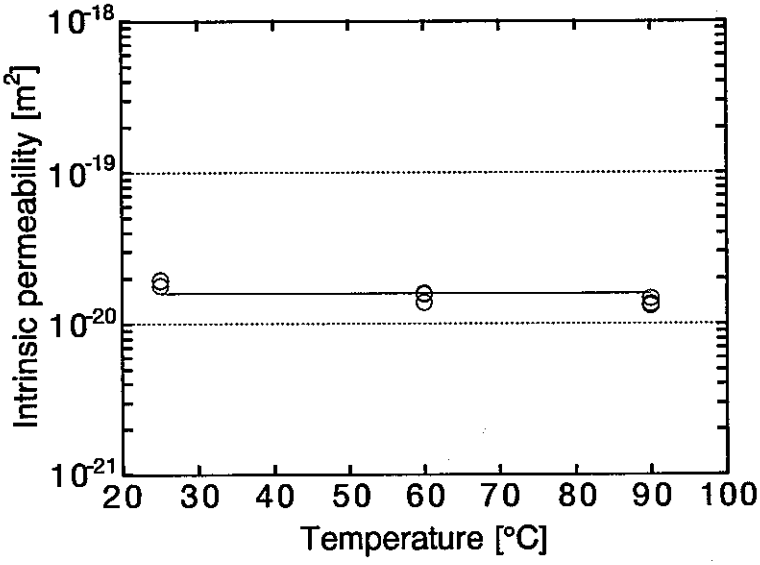

Figure 3.3 Relation between intrinsic permeability and temperature

Table 3.1 Hydraulic conductivity and intrinsic permeability

Temperature	25	60	90
Hydraulic conductivity	2.14E-13	3.31E-13	3.95E-13
[m/s]	2.12E-13	3.22E-13	4.41E-13
	1.96E-13	2.86E-13	4.07E-13
Intrinsic permeability	1.95E-20	1.60E-20	1.32E-20
[m²]	1.93E-20	1.56E-20	1.47E-20
	1.79E-20	1.39E-20	1.36E-20
Mean			1.60E-20

3.1.2 WATER MOVEMENT IN UNSATURATED STATE

(1) WATER MOVEMENT UNDER ISOTHERMAL CONDITION

The water movement in unsaturated bentonite is expressed by the following equation [4].

$$Q = -k\frac{\partial \psi}{\partial z} \tag{3.3}$$

where Q is the flux of water, k is unsaturated hydraulic conductivity and z is the elevation. Total potential of pore water in the bentonite, ψ, is composed of the matric potential, gravity

potential and osmotic potential.

The isothermal infiltration tests were carried out in order to understand the behavior of the water movement in unsaturated bentonite. The compacted bentonite specimens (diameter 20 mm, height 20 mm) were set in stainless steel cells (Figure 3.4) and water was supplied to the specimen from the bottom. The specimen was sliced into 2 mm sections after various infiltration periods. The water content of each section was measured by oven-drying (110°C,24h). The temperature of the experiments was in the range of 25-60°C.

The distributions of the volumetric water content obtained from the infiltration tests for the specimens with the dry density of 1.65 g/cm^3 and the initial water content of 0 % are shown in Table 3.2 and Figure 3.5.

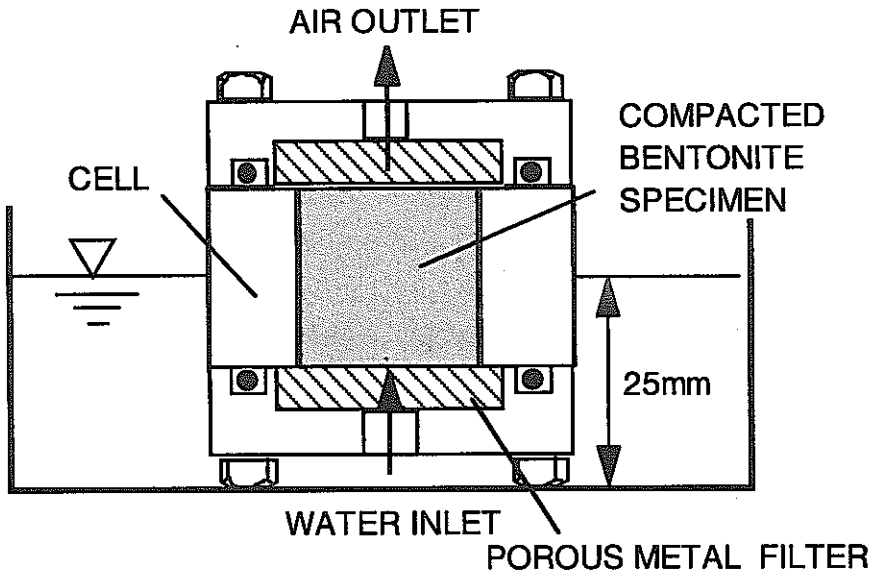

Figure 3.4 Schematic of test apparatus of isothermal infiltration tests

Table 3.2 Volumetric water content (%) obtained from isothermal infiltration tests

T=25°C

Distance* [mm]	Elapsed Time [h]								
	2	4	6	8	16	24	48	72	96
1	31.5	36.6	40.5	38.7	40.4	35.5	54.9	41.2	40.2
3	8.5	13.6	15.7	18.7	22.8	24.3	28.0	32.2	31.5
5	2.5	7.3	9.3	12.1	16.6	18.0	22.9	25.4	27.3
7	1.9	2.9	4.5	6.1	11.3	13.8	18.3	21.1	23.2
9	1.7	2.0	2.7	2.6	7.1	9.5	17.2	19.4	20.5
11	1.7	1.8	2.1	2.1	5.0	6.5	14.5	17.5	19.8
13	1.4	1.6	2.1	2.2	3.4	5.5	11.2	15.8	17.9
15	1.7	1.6	1.6	2.1	2.6	5.0	9.8	14.1	16.2
17	1.0	0.9	2.1	1.4	2.6	3.7	7.2	13.3	16.0
19	1.6	1.3	1.6	2.3	1.8	3.5	6.4	10.3	12.2

T=40°C

Distance* [mm]	Elapsed Time [h]								
	2	4	6	8	16	24	48	72	96
1	34.1	36.7	44.8	39.0	37.4	39.2	44.8	-	-
3	12.4	16.3	20.1	19.1	23.1	24.9	28.4	-	-
5	4.9	9.0	13.1	13.9	17.1	19.4	23.7	-	-
7	2.4	4.5	7.3	8.7	14.5	17.0	21.1	-	-
9	1.7	2.8	4.5	5.9	10.4	14.8	18.5	-	-
11	1.7	1.9	3.0	3.8	7.8	10.8	16.2	-	-
13	1.4	1.4	2.8	2.8	6.7	8.5	15.1	-	-
15	1.4	1.5	2.0	2.6	5.0	6.5	13.7	-	-
17	0.3	1.0	1.6	-	4.3	-	-	-	-
18	-	-	-	1.7	-	5.4	9.1	-	-
19	1.6	0.9	1.3	-	3.7	-	-	-	-

T=60°C

Distance* [mm]	Elapsed Time [h]								
	2	4	6	8	16	24	48	72	96
1	35.2	35.2	40.0	31.2	49.3	48.5	41.9	-	-
3	16.9	18.2	19.0	20.3	23.3	26.1	26.8	-	-
5	9.4	12.1	14.9	17.1	19.2	20.1	22.6	-	-
7	5.5	7.6	11.0	13.4	17.1	18.8	19.4	-	-
9	3.4	4.7	6.8	9.4	14.9	14.7	17.8	-	-
11	2.7	3.2	5.3	7.6	12.5	14.1	16.3	-	-
13	2.3	2.2	3.6	6.5	9.5	12.1	15.6	-	-
15	1.3	1.5	3.0	4.9	8.3	9.0	11.9	-	-
17	1.4	-	-	-	-	-	-	-	-
18	-	1.1	1.4	3.3	5.2	6.5	8.8	-	-

* Distance from the bottom

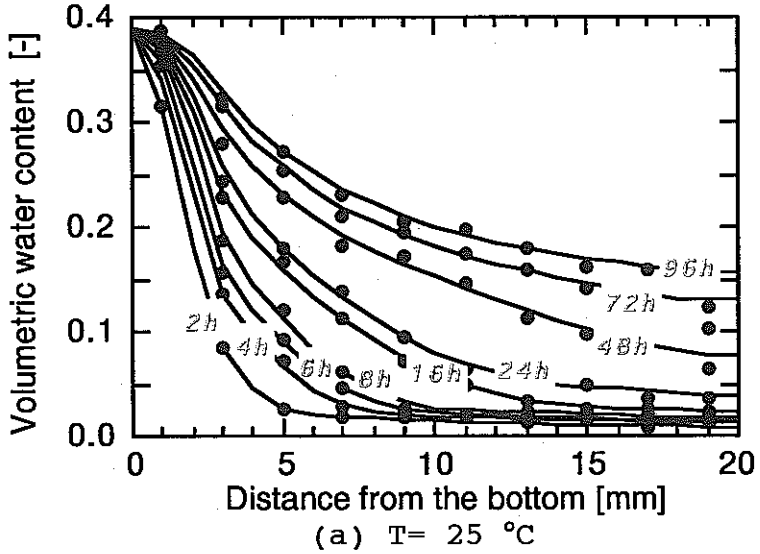

(a) T= 25 °C

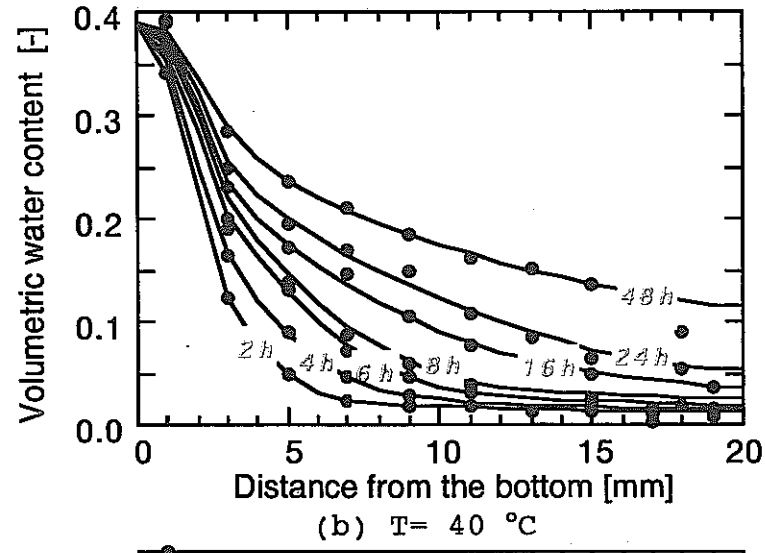

(b) T= 40 °C

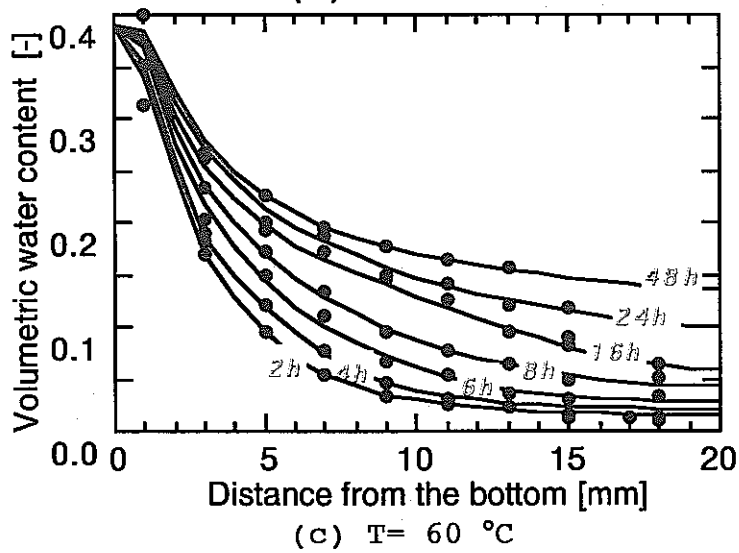

(c) T= 60 °C

Figure 3.5 Distribution of volumetric water content

Since the effects of the gravity and osmotic potentials are negligible in case of the bentonite [5], the water flux is given by

$$Q = -k\frac{d\varphi}{d\theta}\frac{\partial\theta}{\partial z} = -D_\theta\frac{\partial\theta}{\partial z} \tag{3.4}$$

in which

$$D_\theta = k\frac{d\varphi}{d\theta} \tag{3.5}$$

where D_θ is the water diffusivity, θ is the volumetric water content and φ is the matric potential. Then the water diffusivity is calculated by the following equation based on the distribution of volumetric water content obtained by infiltration experiment [5]

$$D_\theta = \frac{\int_{z_i}^{l}\left(\theta_{t=t_2} - \theta_{t=t_1}\right)dz}{\frac{1}{2}\left\{\left(\frac{\partial\theta}{\partial z}\right)_{z=z_i}^{t=t_2} + \left(\frac{\partial\theta}{\partial z}\right)_{z=z_i}^{t=t_1}\right\}} \times \frac{1}{t_2 - t_1} \tag{3.6}$$

where t is infiltration time, l is the length of the specimen and z_i ($0 \le i \le l$) is distance from the bottom of the specimen.

The water diffusivities calculated from the distributions of the volumetric water content are shown in Figure 3.6. The water diffusivity depends on the volumetric water content, and can be expressed as U-shaped curves. And the minimum value of the water diffusivity increases with the increment of the temperature. It is assumed that the relationship between water diffusivities and volumetric water content is expressed as the sum of two hyperbolic functions, as shown in the following equation.

$$D_\theta = \frac{a_1(\theta - \theta_{sat})}{(\theta - b_1)(b_1 - \theta_{sat})} + \frac{a_2\theta}{b_2(\theta - b_2)} \tag{3.7}$$

where θ_{sat} is the volumetric water content in saturated state, a_i and b_i are constant. The relations with these parameters obtained

from the calculation are summarized in Table 3.4 and are presented by dotted lines in Figure 3.6.

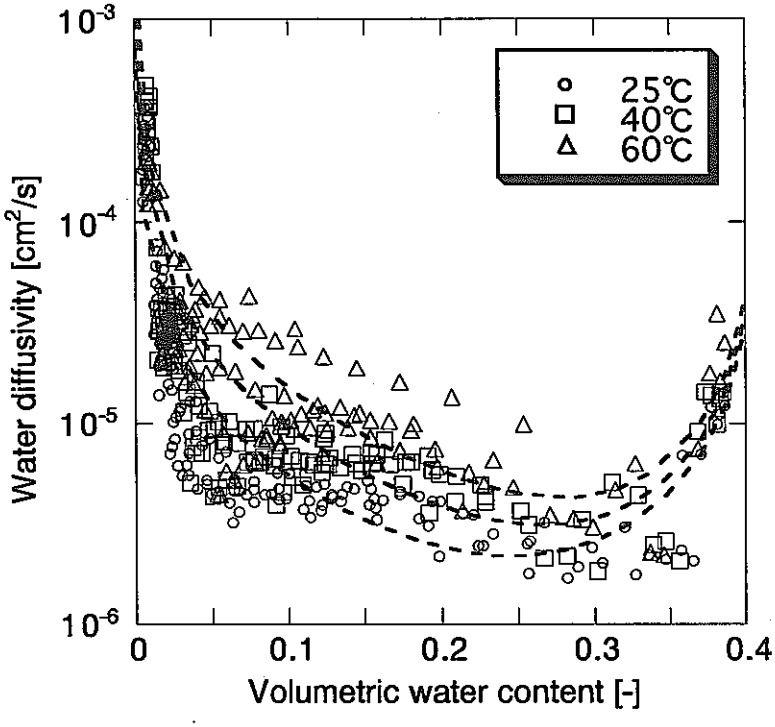

Figure 3.6 Water diffusivity

Table 3.3 Parameters in the equation (3.7)

Parameter	Values
a_1	3.68E-8 T-2.08E-7
a_2	-3.58E-9 T+2.19E-7
b_1	-0.001
b_2	0.41
θ_{sat}	0.389

T ; Temperature

(2) WATER MOVEMENT UNDER THERMAL GRADIENT CONDITION

The infiltration tests under thermal gradient condition were carried out in order to understand the behavior of the water movement in unsaturated bentonite. The compacted bentonite specimens (diameter 50 mm, height 100 mm) packaged in a food wrap film were set in a apparatus, named KID-BEN for small sized coupled thermal-hydraulic-mechanical test (Figure 3.7). The cell of KID-BEN is made of bakelite which is one of thermosetting resin and has air layer in order to enhance thermal-insulating effects. The cooling and heating portions are composed of copper plates and thermostat with circulation system, UNIACE UA-10S manufactured by EYELA. The K-type sheathed thermocouples (JIS C 1602) manufactured by TOKO THERMOSCIENCE CORP. were put in the holes drilled in the surface of the specimen side. The specimen was sliced into 20 mm sections after various infiltration periods. The water content of each section was measured by oven-drying (110°C,24h). The test condition are summarized in Table 3.4.

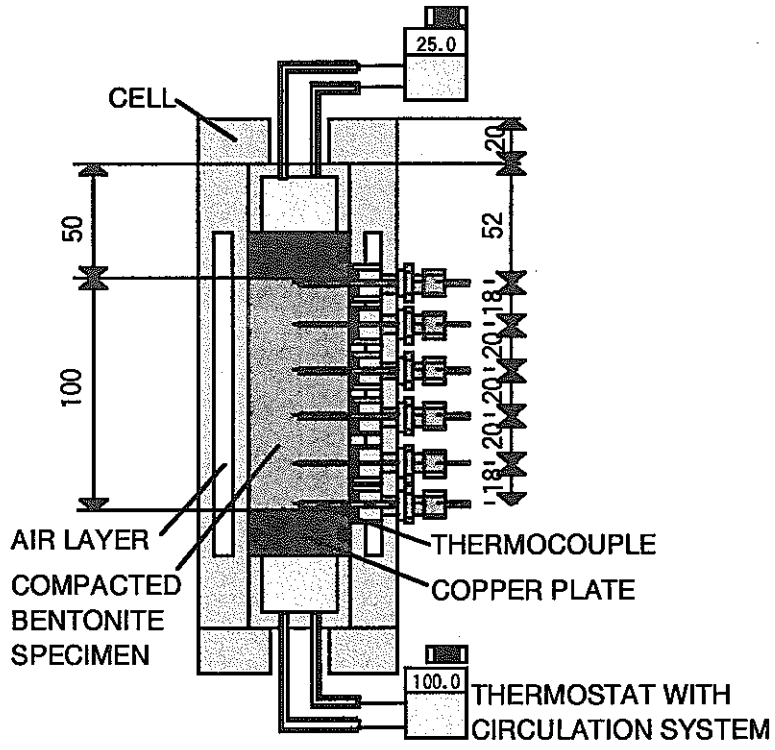

Figure 3.7 Schematic of test apparatus of KID-BEN

The distributions of the volumetric water content and temperature after 96 hours obtained from the infiltration tests under thermal gradient are shown in Table 3.5, Figures 3.8 and 3.9

Table 3.4 Conditions for infiltration tests under thermal gradient

Test No.		1	2	3
Dry density (g/cm³)		1.65	1.65	1.65
Initial volumetric water content (%)		26.5	26.5	26.5
Temperature gradient (°C/cm)		1	3	5
Temperature (°C)	Upper side	25	25	25
	Bottom side	35	55	75
Heating time (hour)		96	96	96

Table 3.5 Distributions of the volumetric water content and temperature

Distance[1] [mm]	Test No. 1		2		3	
	VWC[2] (%)	TEMP[3]. (°C)	VWC[2] (%)	TEMP[3]. (°C)	VWC[2] (%)	TEMP[3]. (°C)
2		34.9		53.2		72.3
5	25.311		21.598		15.592	
15	25.691		23.513		18.067	
20		31.9		44.3		57.6
25	26.202		25.146		19.800	
35	26.417		25.889		23.100	
40		30.1		38.0		46.5
45	26.450		26.681		26.351	
55	26.499		27.093		28.578	
60		28.3		33.2		38.2
65	27.027		28.116		30.690	
75	27.060		28.545		31.268	
80		27.0		29.4		31.7
85	27.143		28.677		31.763	
95	27.390		29.799		33.643	
98		26.0		26.3		26.7

1) Distance from the bottom
2) Volumetric water content
3) Temperature

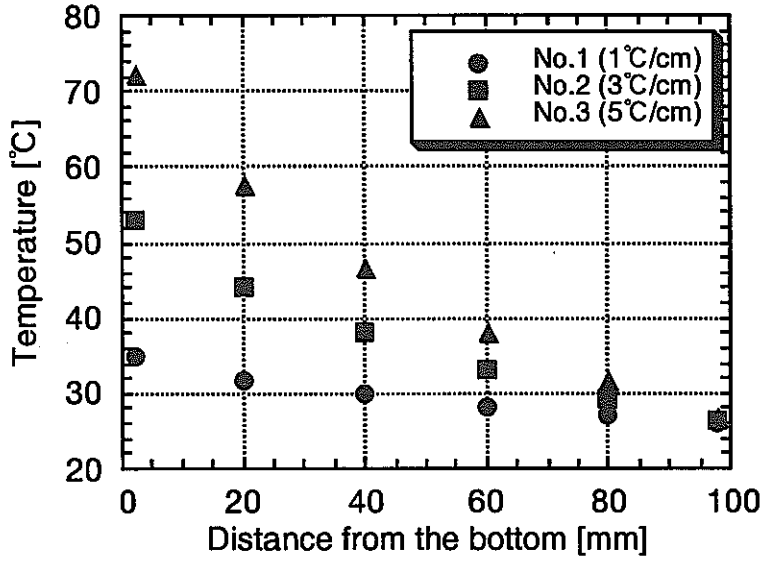

Figure 3.8 Distribution of temperature obtained from the infiltration tests under thermal gradient

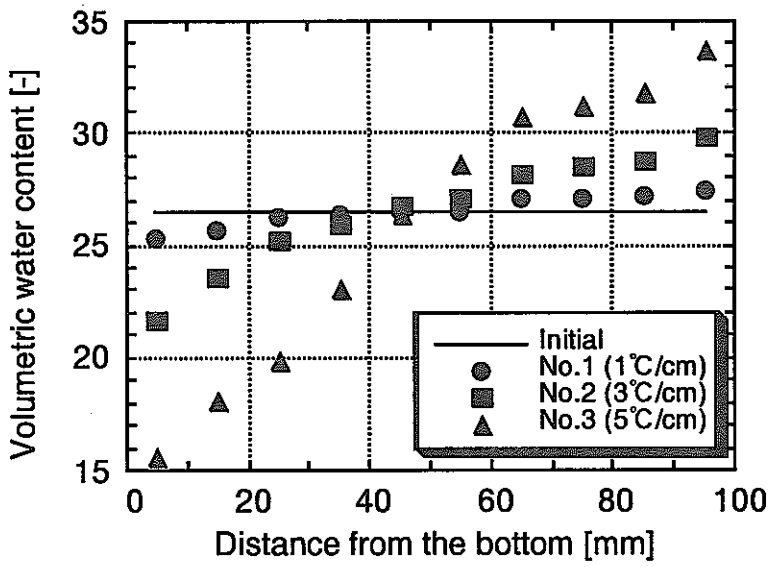

Figure 3.9 Distribution of volumetric water content obtained from the infiltration tests under thermal gradient

(3) WATER POTENTIAL

The water potential ψ is calculated from relative humidity P/P_0 by the following equation [6]

$$\psi = \frac{RT}{M} ln \frac{P}{P_0} \tag{3.8}$$

where M is the molecular weight of water, R is the gas constant, T is the absolute temperature, P is the vapor pressure of sample and P_0 is saturated vapor pressure.

The water potential of bentonite specimens with various initial water contents was measured by a thermocouple psychrometer (WESCOR INC) in a thermostat (Figure 3.10). The diameter of the specimens was 13 mm and the height was 9 mm. The psychrometer senses the relative humidity of moist air in equilibrium with the liquid phase in the bentonite. From the measured relative humidity, the water potential can be obtained by equation (3.8). The water content of the specimens were measured by oven-drying (110°C, 24 h). Then the water retention curve was obtained by plotting the water potential as a function of water content. The temperature of the experiment were 25, 40 and 60°C.

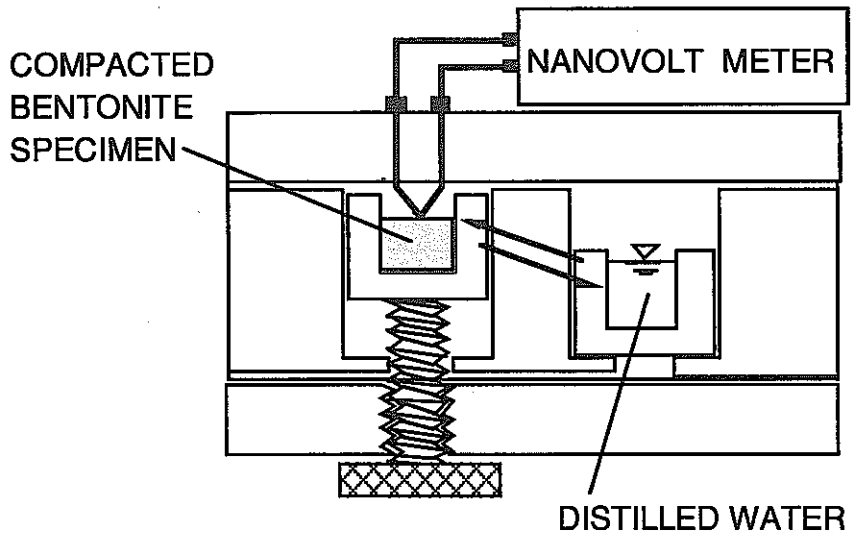

Figure 3.10 Schematic of thermocouple psychrometer

The water retention curve determined from the psychrometric measurements are shown in Table 3.6 and Figure 3.11 in which the water potential is expressed as suction in MPa. The dependence of the water content on temperature is not large in the condition of temperature ranging from 25° to 60°C. The dotted line of the water retention curve in Figure 3.11 can be described as the following equation.

$$\psi = 128.9\exp\left(-1.62\times10^{-2}\omega^{2}\right)+21.573\omega^{-0.786} \qquad (3.9)$$

Table 3.6 Data on water retention curve

WC*	SUCTION (MPa)			WC*	SUCTION (MPa)			WC*	SUCTION (MPa)		
(%)	T=25°C	T=40°C	T=60°C	(%)	T=25°C	T=40°C	T=60°C	(%)	T=25°C	T=40°C	T=60°C
0.15	192			6.40			62.3	16.21	3.21		
0.22		209		6.42		64.8		16.53			3.99
0.27	185	208		7.62	47.1			16.76		3.69	
0.62			192	7.69			56.3	17.21	2.84		
0.84			170	7.73		57.6		17.46		3.4	
1.14		156		8.90			49.2	17.88			3.72
1.17	143			8.95	40.3			18.14	2.57		
1.40			164	9.00		49.4		18.60	2.19		
1.63	137			10.19	27.9			18.62		2.9	
1.63		148		10.28			33.3	18.79	2.06		
1.91			156	10.46		35		19.16			3.22
2.26	127			10.94	22.9			19.69		2.49	
2.33		128		11.28		28.3		19.72	2.08		
2.59			138	11.38			26.8	20.83			2.91
2.92	116	123		11.87	17.1			21.32		2.14	
3.09			126	11.93			20.4	21.72	1.8		
3.79		101		12.02		20.4		22.39			2.47
3.83	96.7			13.34			9.9	22.98			2.28
4.02			110	13.71	7.71	8.76		23.18		1.87	
4.04		83		14.31		5.98		23.39	1.6		
4.77	79.4			14.40	4.92			23.47	1.58		
4.85			91	15.06			5.39	23.78		1.79	
5.40			70	15.20	4.03			24.34	1.57		
5.59	56			15.34		5.07		24.46		1.77	
5.65		69.7		15.93			4.76	-	-	-	-
6.34	51.5			16.18		3.94		-	-	-	-

* Water content

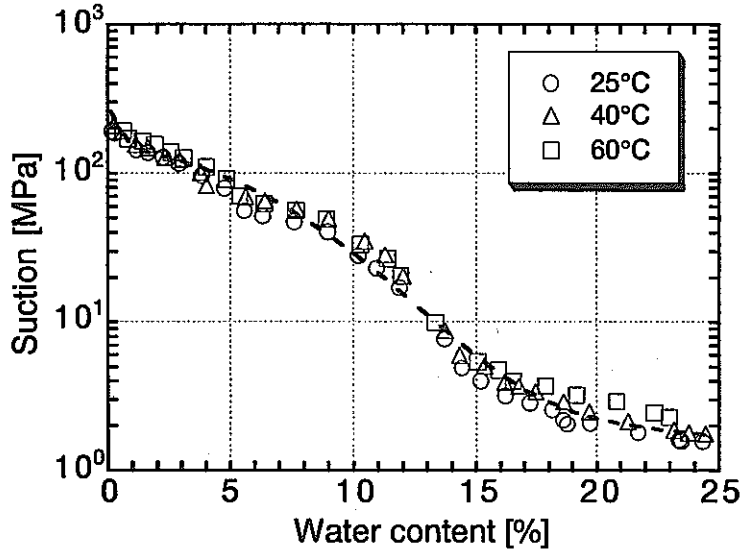

Figure 3.11 Water retention curve

(4) PARAMETER

The principal properties of the bentonite regarding the water movement on unsaturated state are described in the above sections. The some models regarding the water movement on unsaturated clay are proposed by many researchers, for example Philip and de Vries [7], van Genuchten [8] and so on. It is necessary to estimate some parameters used in each model.

3.2 THERMAL PROPERTIES

3.1.1 THERMAL CONDUCTIVITY

The heat transport is described using Fourier's law.

$$C_p \rho \frac{\partial T}{\partial t} = \lambda_{ii} T_{,ii} \qquad (3.10)$$

where C_p is the specific heat, ρ is the density, λ_{ij} is the thermal conductivity tensor, T is temperature, and t is time.

Thermal conductivity of bentonite with a dry density of 1.65 g/cm^3 was measured using QTM (Quick Thermal Conductivity Meter) based on the hot wire method (Figure 3.12). The probe of known thermal conductivity in contact with the specimen is heated and the temperature changes of the specimen are measured. The thermal conductivity of bentonite λ_p is calculated by the following equation.

$$\lambda_p = K\frac{I^2 \ln(t_2/t_1)}{(T_2/T_1)} - H \qquad (3.11)$$

where I is the current, K and H are the probe constant, t is the sampling time and T is temperature. The conditions of the experiment were water content in the ranges of 0-22.84%, dry density of 1.65 g/cm^3 and temperature of 25°C.

Table 3.7 and Figure 3.13 show thermal conductivity at various water content. The thermal conductivity increases as water content increases.

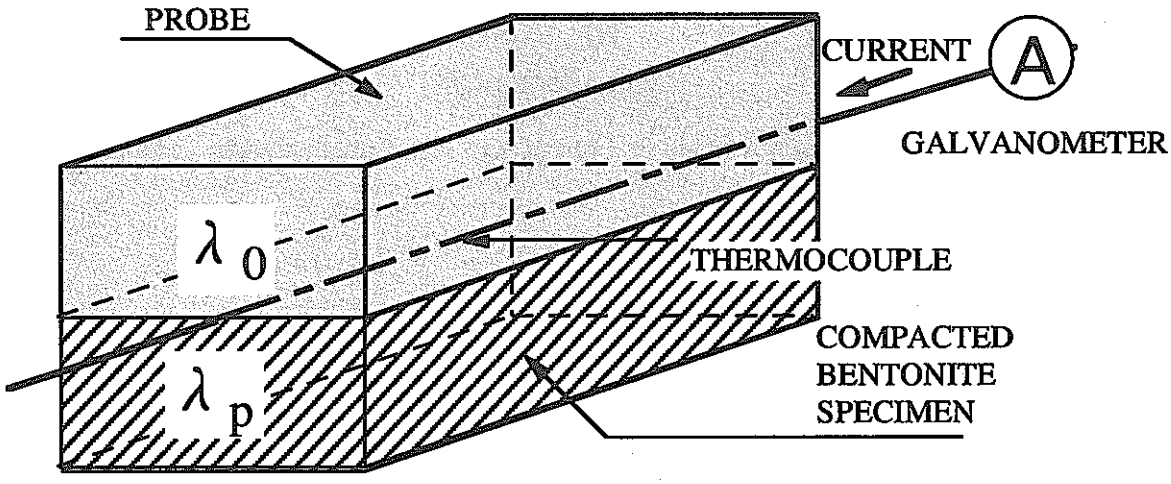

Figure 3.12 Schematic of QTM

Table 3.7 Data on thermal conductivity

Water content (%)	Thermal conductivity (W/m°C)
0.00	0.558
5.04	0.716
9.96	0.954
14.81	1.245
19.63	1.442
22.84	1.689

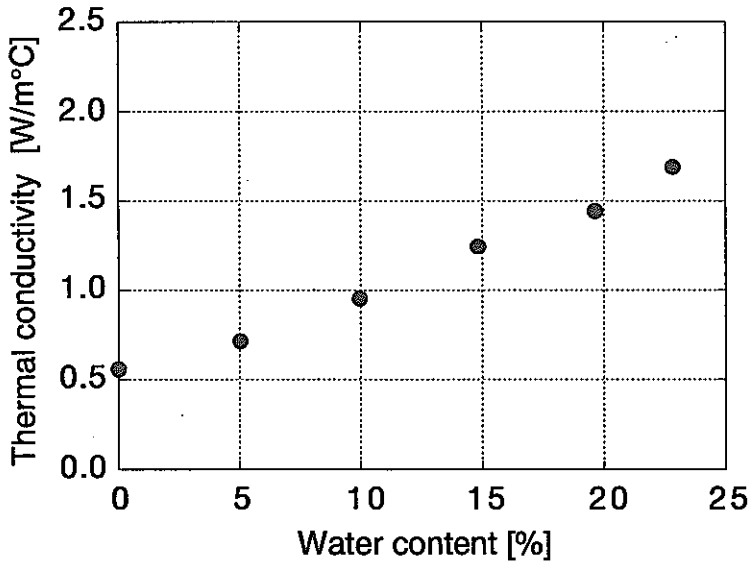

Figure 3.13 Thermal conductivity at various water content

3.3 MECHANICAL PROPERTIES

3.3.1 UNCONFINED COMPRESSION TEST

The COMPUTER CONTROL SYSTEM SHIMADZU AUTOGRAPH was used for the unconfined compression test. This system shown in Figure 3.14 was called Model AG-10TB. The maximum compressive stress till a failure of the specimen was the unconfined compressive strength. The secant modulus at 50% of the peak strength was the Young's modulus. The axis displacement controls were adopted as control

mode for this test and the axis compression displacement rate was set to be 0.1 mm/min. The specimen was 5 cm in diameter and 10 cm in height and the dry density was 1.65 g/cm^3. The conditions of the experiment were water content in the range of 0-23.58% and temperature of 25°C.

The unconfined compressive strength and Young's modulus obtained from unconfined compression test are summarized in Table 3.8, Figure 3.15 and 3.16. It is indicated that both have the maximum values near the water content of 10 %.

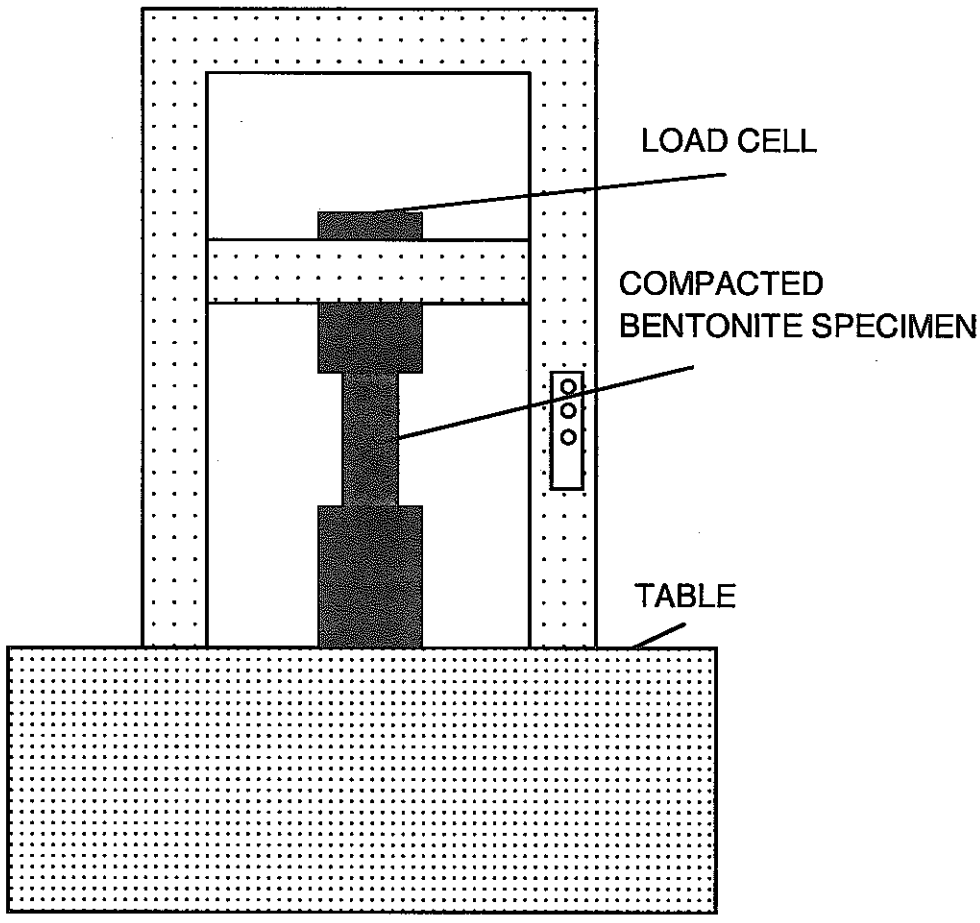

Figure 3.14 Triaxial testing system

Table 3.8 Results of unconfined compression test

Water content (%)	Unconfined compressive strength (MPa)		Young's modulus (x100 MPa)	
5.25	0.91	1.00	1.35	1.38
10.05	1.15	1.21	2.15	2.97
14.96	0.82	0.87	1.42	1.47
19.82	0.55		0.33	
23.58	0.46		0.13	

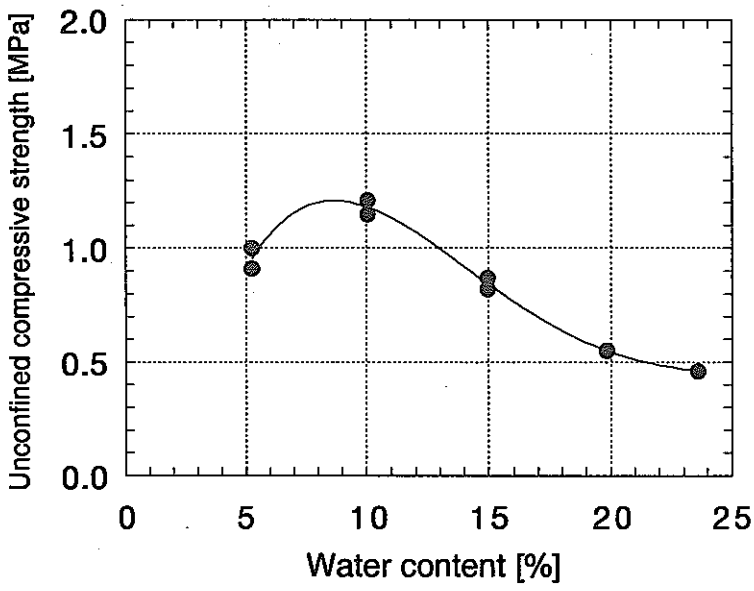

Figure 3.15 Unconfined compressive strength

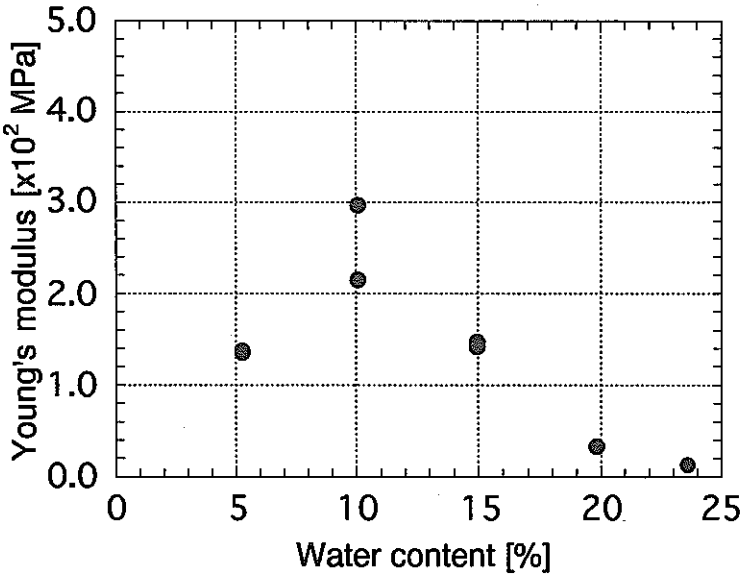

Figure 3.16 Young's modulus

3.3.2 SWELLING STRESS

A compacted bentonite swells with water uptake and the stress builds up on a restraint boundary surfaces under restraint condition, which is called the swelling stress.

Three samples were compacted uniaxially and statically to a dry density of 1.65 g/cm^3 and water content of 16 % in rigid stainless steel cells, shown in Figure 3.17, for swelling stress tests. The diameter of the cells was 20 mm and the thickness of the compacted specimens was 20 mm. Distilled water pressurized by compressed air was supplied into the cell through the porous metal filter of which the pore diameter was 5 μm and teflon filter of which the pore diameter was 2 μm. The swelling stress was determined by load cells manufactured by KYOUWA, type LC-FH500K, maximum capacity 500 kg, temperature range of -10~150 ℃ and accuracy for temperature of 0.01 %/°C. The pressure of the compressed air was maintained at 0.1 MPa during the tests. In this study, the following heating procedure for each bentonite specimen with a thermostat was adopted; 25°C →60°C →90°C.

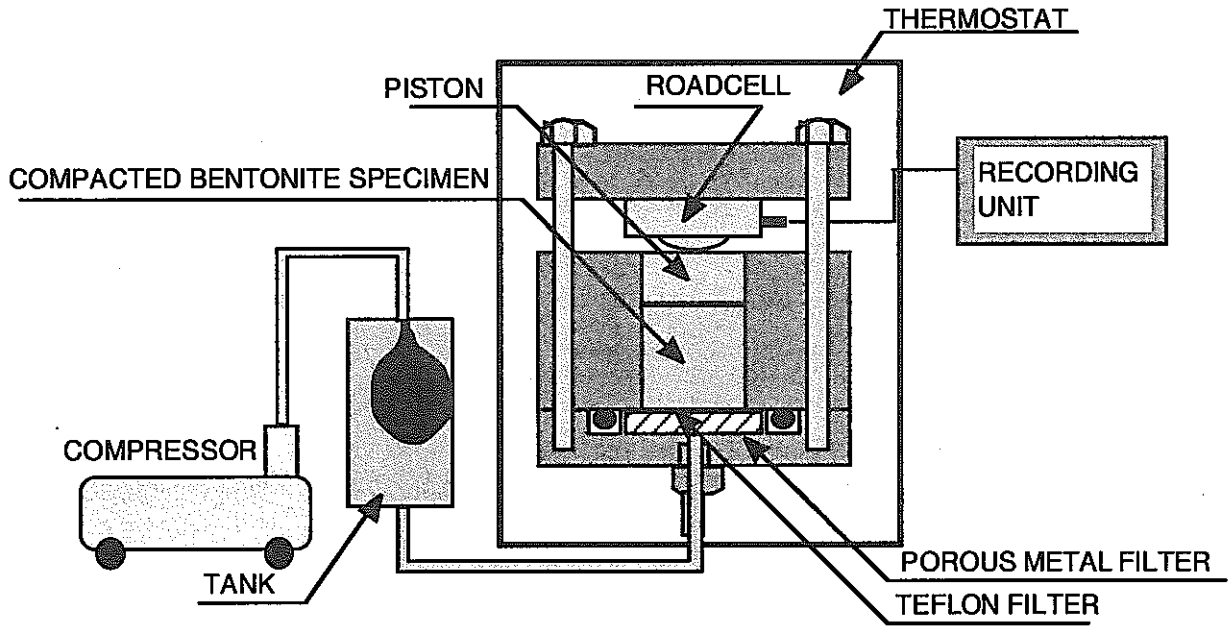

Figure 3.17 Schematic of test apparatus of swelling stress test

Figure 3.18 shows the swelling stress change with time. The swelling stress changed greatly at 105 and 140 days elapsed, because power failure occurred for about 2 days and temperature decrease. It is indicated that the swelling stress decreases with increases in temperature.

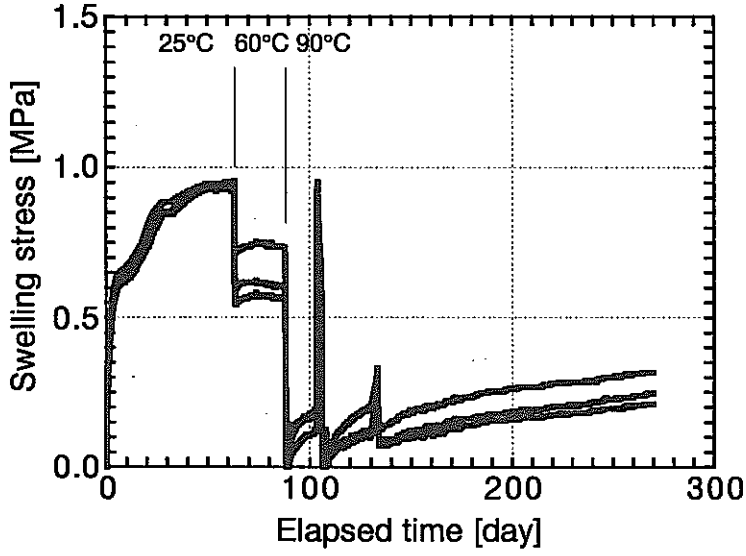

Figure 3.18 Swelling stress with elapsed time

3.3.3 DRYING SHRINKAGE

The test for shrinkage parameters of compacted bentonite were carried out in order to observe the volume change and crack by the volume change of compacted bentonite. The bentonite was compacted uniaxially and statically to a diameter of 30 mm, a height of 60 mm and a dry density of 1.65 g/cm^3 with the five kinds of water contents. The diameter, height and weight of the specimens were measured before and after oven-drying (110°C,24h). The repetition rate of test for each water content were three times.

Figure 3.19 shows the photograph of the bentonites after oven-drying. The photograph indicates that cracks occurs in the samples at water contents of 19.19 and 22.90 %.

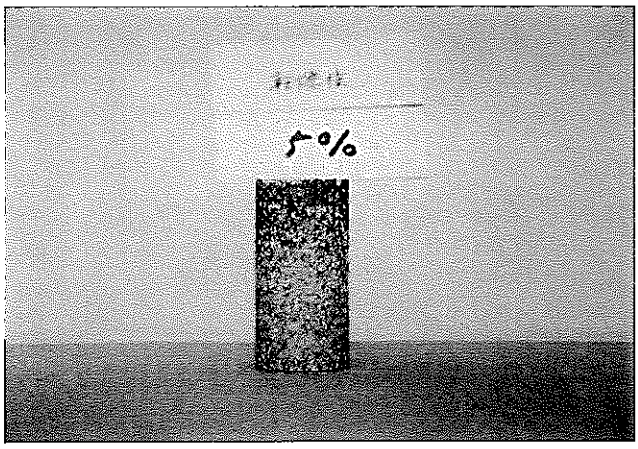

(a) Initial water content = 5.12

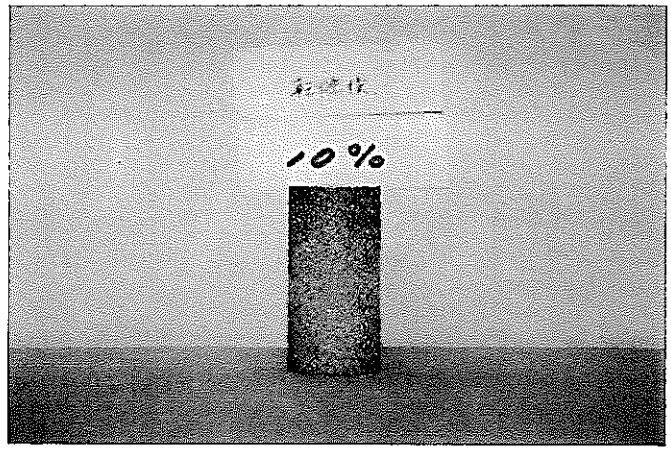

(b) Initial water content = 9.91

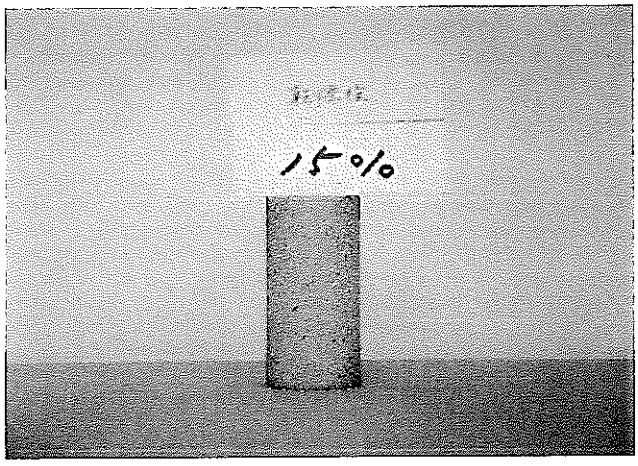

(c) Initial water content = 14.59

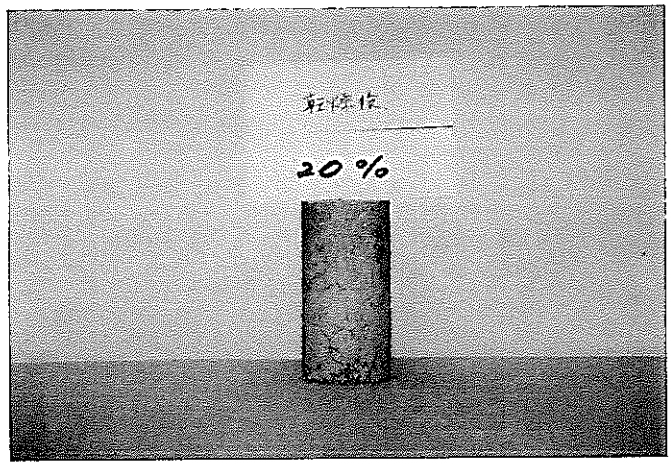

(d) Initial water content = 19.19

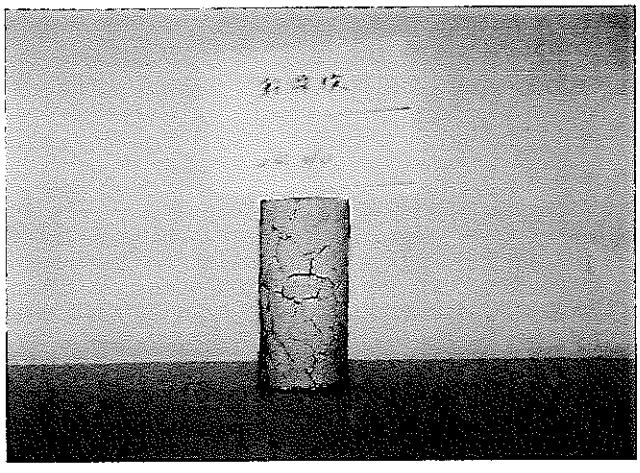

(e) Initial water content = 22.90

Figure 3.19 Photograph of the bentonites after oven-drying

The relation between the volume change V/V_0x100, where V is the initial volume and V_0 is the volume after over drying, and water content ω is shown in Figure 3.20. The volume change increases with water content.

The shrinkage limit ω_s, shrinkage ratio R, volume shrinkage ratio C and linear shrinkage L_s are defined by following equations.

$$\omega_s = \omega - \frac{(V - V_0)\rho_w}{m_s} \times 100 \qquad (3.12)$$

$$R = \frac{m_s}{V_0 \rho_w} \qquad (3.13)$$

$$C = (\omega - \omega_s)R \qquad (3.14)$$

$$L_s = \left(1 - \sqrt[3]{\frac{100}{C+100}}\right) \times 100 \qquad (3.15)$$

where m_s is the dry mass and ρ_w is the density of water. The above parameters obtained are summarized in Table 3.9. The relation between linear shrinkage and water content as shown in Figure 21 can be described as following equation.

$$L_s = e^{0.122\omega} + 0.146 \qquad (3.16)$$

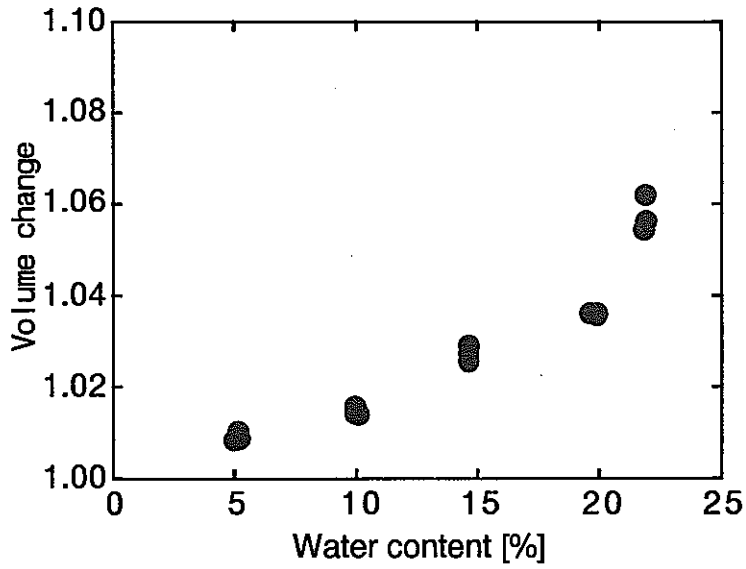

Figure 3.20 Relation between the volume change and water content

Table 3.9 Shrinkage parameters of compacted bentonite

Water content [%]	Shrinkage limit [%]	Shrinkage ratio [-]	Volume shrinkage ratio [%]	Linear shrinkage [%]
5.12	4.56	1.63	0.91	0.30
9.91	9.11	1.65	1.32	0.44
14.59	13.00	1.68	2.67	2.60
19.19	17.69	1.69	2.40	2.34
22.90	18.59	1.74	7.50	6.98

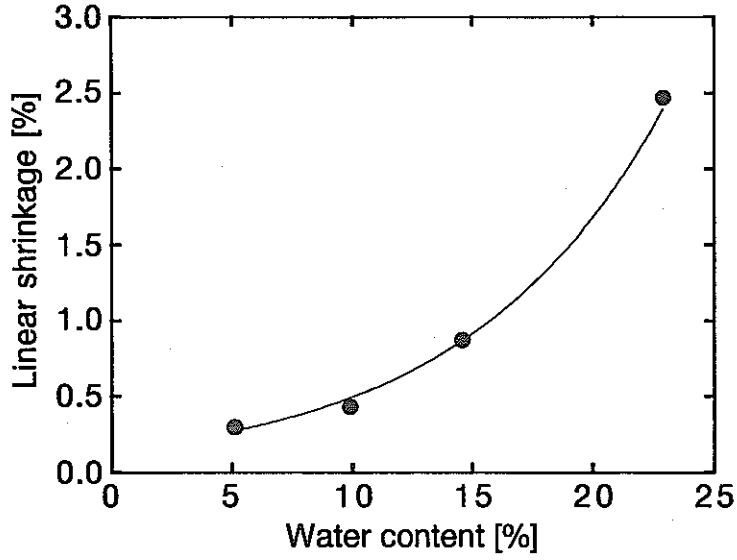

Figure 21 Relation between linear shrinkage and water content

4 SUMMARY

In order to understand and to model T-H-M behavior of bentonite in the T-H-M experiment at the Kamaishi mine, measurements of hydraulic, thermal and mechanical properties on the BENTONITE OT-9607 at laboratory were carried out.

Temperature dependence of saturated hydraulic conductivity of the OT-9607 is examined by the intrinsic permeability concept

and the dependence is concluded to be due to changes in the viscosity and density of pore water.

For the water movement in unsaturated state, the temperature dependence of the water diffusivity for compacted bentonite is observed. However, the dependence of the water potential on temperature is not large in the condition of temperature ranging from 25° to 60°C.

The thermal conductivity has the water content dependence and increases as water content increases.

The maximum unconfined compressive strength and Young's modulus are obtained near the water content of 10 %.

The swelling stress decreases with increases in temperature.

The cracks due to drying shrinkage occurs in the samples at water contents of 19.19 and 22.90 %.

The several models for the properties of bentonite are proposed by many researchers. It is necessary to estimate several parameters to fit each model, when the properties are used as input data in a numerical calculation.

5 ACKNOWLEDGMENTS

The authors are grateful to Mr.T.Kanno of PNC for providing valuable comments and suggestions.

REFERENCES

[1] Fujita,T., Sugita,Y. ,Sato,T., Ishikawa,H. and Mano,T.; PLAN OF COUPLED THERMO-HYDRO-MECHANICAL EXPERIMENT AT THE KAMAISHI MINE, PNC Technical Report, PNC TN8020 94-005, 1994.

[2] Ishikawa,H., Amemiya,K., Yusa,Y. and Sasaki,N.; Comparison of fundamental properties of Japanese bentonite as buffer material for waste disposal, Proc. 9th International Clay Conference, Strasbourg, France, 1989.

[3] Bear,J.; *Hydraulics of Groundwater*, McGraw-Hill Publishing Company, 66-67, 1979.

[4] Nakano,M., Amemiya,Y. and Fujii,K.; Saturated and unsaturated hydraulic conductivity of swelling clays, *Soil Science*, 141, 1, 1986.

[5] Nakano,M., Amemiya,Y., Fujii,K., Ishida,T. and Ishii,Y.; Infiltration and volumetric expansion in unsaturated clay, (in Japanese) *Trans Jpn. Soc. Irrig. Reclam..*, 100, 8-16, 1982.

[6] Smith,K. and Nullins,C.; *Soil Analysis - Physical Methods*, Marcel Dekker Inc., 98, 1991

[7] Philip,J. R. and de Vries,D.A.; Moisture movement in porous materials under temperature gradients, *Am. Geophys. Union Trans*, 38, 2, 1957.

[8] van Genuchten,M. Th.; A closed-form equation for predicting the hydraulic conductivity of unsaturated soils, *Soil Sci. Soc. Am. J*, 44, 892-898, 1980.